Synthesis and Characterization of Pure and Nickel Doped SrTiO₃Nanoparticles via Solid State Reaction Route

G.Viruthagiri*, P.Praveen, S.Mugundan, E.Gopinathan

Department of Physics, Annamalai University, Annamalai Nagar-608 002, Tamilnadu, India

ABSTRACT

Synthesis of non-doped and Ni (0.5% and 1% atom) doped perovskite type SrTiO₃ (STO) was carryout by solid-state reaction route. The influence of doping amount of Ni on STO was investigated. The phase transformation was confirmed by X-ray diffraction (XRD) analysis. All the compositions synthesized have cubic structure similar to undoped SrTiO₃. Average grain sizes of pure and Nickel doped samples were 42.76 nm and 59.41 nm respectively. The functional groups of the samples were identified by Fourier transform infrared spectroscopy (FT-IR).The UV-Vis diffuse reflectance spectra (DRS) revealed that the absorption maximum decreases with the particle size and band gaps were calculated using the formula $E_g = hc/\lambda$ eV and are 3.67 eV, 4.13 eV and 4.46 eV respectively for non-doped and Ni doped SrTiO₃ nanoparticles. Microstructures (surface morphology) were characterized using scanning electron microscopy (SEM).

Keywords: Ni doped SrTiO₃; X-ray diffraction; FT-IR; UV-Vis-DRS; band gap; SEM

1. INTRODUCTION

Nano structured materials have been fascinating the world of science and technology during the last 15 years because of their tremendous possibilities in generating novel shapes, structures, and the unusual phenomena associated with these materials. The characteristic length of these materials (at least one length) lies between 1–100 nm. This makes the properties of matter within this length scale significantly different from individual atoms or molecules and from bulk materials. Nano particles exhibit unique electronic, magnetic, optical, photonic, and catalytic properties, and their size is ideal for use as building blocks, which includes metals, semiconductors, core-shell nanostructure, and organic polymeric materials [1]. The properties of nanomaterials are influenced by the presence of a significant number of surface atoms and by the quantum confinement effect of the electronic states. The potential applications for nanostructured oxide materials include paint pigments, cosmetics, pharmaceuticals, medical diagnostics, catalysts and supports, membranes and filters, batteries and fuel cells, electronics, magnetic and optical devices, flat panel displays, biomaterials, structured materials and protective coatings. Nano particle reactivity is being done today because of the scarcity of equipment allowing an open field for development of this technology.

Strontium titanate has been studied extensively for technological applications as well as for basic science due to its electronic properties, chemical stability, and structural behavior. Strontium titanate

(SrTiO₃) has been used for water splitting, because they provide a higher photo potential than TiO₂ and facilitate hydrogen and oxygen formation. Perovskites are also observed to be useful for the degradation of organic compounds in place of conventional photo catalysts, such as TiO₂. Perovskites have the general formula (ABO₃). The perovskite structure provides the flexibility to vary the composition of the A and B sites and/or incorporate a combination of cations at the A and B sites to form substituted perovskites. In an ABO₃ Perovskite, varying the stoichiometry or doping with a cation of a different valence state can, in principle, change the electronic properties. Therefore, unlike TiO₂, one can control the composition and size of the constituent cations and can potentially alter the electronic structure of a perovskite semiconductor. Some typical general formulas of substituted perovskites are AxA'1-xBO₃, ABxB'1-xO₃, etc. Therefore, doping with different cations (A' or B') offers the potential to tailor the basic structure and hence the electronic and catalytic Properties of substituted perovskites [2].

Strontium titanate (SrTiO₃) is an excellent example of a perovskite structure exhibiting a wide range of defect chemistry that can illustrate the influence of different factors on electronic conductivity. It exhibits n-type semi conducting behavior when donor doped and or exposed to a reducing atmosphere. The defect chemistry and its effect on conductivity in donor-doped SrTiO₃ have been extensively reported in literature [3],[4]; the extra

---

Corresponding Author:
E-mail address: gvgiri2002@gmail.com
Phone:+91-9486223626

positive charge of the donor needs to be compensated either by strontium vacancies (ionically) in oxidizing atmospheres or conduction electrons provided by the Ti^{4+} reduction to Ti^{3+} in reducing atmospheres. Increasing attention is given to A-site deficient strontium titanate (XSTA, where X is a trivalent metal cation) anodes as this compositional approach can lead to more conductive phases than the stoichiometric ones, at the same oxygen partial pressure. In these formulations donor ions are compensated by strontium vacancies.

Another way to improve the conductivity of $SrTiO_3$ based materials is the replacement of titanium on B-site of the perovskite with cations such as nickel. Perovskites play a highly important role in electro ceramics technology as well as in basic solid state chemistry. In this group of materials, $SrTiO_3$ is an excellent model material for study in mixed conduction and oxygen incorporation as well as boundary effects, since its defect chemistry is well established [2,5,6]. We now have a quantitative set of the relevant equilibrium constants for pure and acceptor doped material as a function of T (Temperature), PO (Partial oxygen) and doping level as well as of the mobility of ionic and electronic charge carriers.

In commercial multilayer ceramic capacitors (MLCs), perovskite structure titanates are frequently used as high permittivity dielectrics. Alkaline earth titanates like $BaTiO_3$, $SrTiO_3$ etc are widely used in microelectronic devices due to their excellent dielectric properties and high thermal stability. $SrTiO_3$, a technologically highly important class of perovskite material, is used in PTC resistors, capacitors and sensors [7]. Important applications of $SrTiO_3$ areas substrates for the hetero epitaxial growth of high Tc superconductors [8], in multi-layer capacitors [9] and DRAM devices etc. Ceramic oxide-based materials like $SrTiO_3$ contain electro-active intra granular (bulk) and inter granular (grain boundary) regions, whose properties depend on the close control of microstructure–stoichiometric relationships. Grain boundaries play an important role in the electrical properties of a variety of ceramic materials and components. In a broad range of ceramics, this shows ionic conduction, mixed ionic–electronic conduction or electronic conduction, grain boundaries act as barriers for the cross transport of the charge carriers. Often, the barrier character of the grain boundary (GB) is especially pronounced in the low temperature regime. In this regime, perovskite type titanates such as $BaTiO_3$, $SrTiO_3$ etc are employed as high permittivity dielectrics for capacitor applications. At elevated temperatures (i.e. well above the Curie temperature), the

$BaTiO_3$ based ceramics gave clear evidence for GB layers of high resistance, which is interpreted as a Schottky-type depletion space charge effect. For most of the above applications, the titanates must be net acceptor doped to prevent semi conduction in the ceramics. The high insulation resistance of MLC components is caused mainly by the fact that grain boundaries (GBs) in the dielectric ceramic act as high resistive barriers for the cross transport of charge carriers. Often, under high temperatures and high voltage fields, these resistive grain boundary barriers are reduced and that give rise to substantially field-enhanced leakage currents through the components.

That is the reason why detailed dielectric studies, especially at GB barrier interface are important for the perovskite-type titanates. Acceptor, e.g. Ni-doped $SrTiO_3$, is a mixed conductor of oxygen vacancies and electron holes. The grain boundary properties of acceptor doped $SrTiO_3$ have already been investigated by impedance spectroscopy on polycrystals and bi-crystals [10], in time dependent voltage stage measurements by simulations [11], using micro-contact measurements etc. Acceptor doped $SrTiO_3$ is again selected as our main material because it shows a defect and crystal structure very similar to $BaTiO_3$, which still is the most important ceramic in the ceramic industries. In contrast to $BaTiO_3$, $SrTiO_3$ is not ferroelectric over the complete temperature range of technical interest. For our purpose, this is beneficial since the ferroelectric behaviour superimposes an additional degree of complexity by significantly affecting the polarization and charge transport in the material. Acceptor doped $SrTiO_3$ which is the core of the present work, the aims to describe the effect of acceptor concentration on microstructure and electrical properties of the ceramic at elevated temperatures [2,12]. In the synthesis of multi component oxide powders such as $SrTiO_3$, chemical solution methods offer several advantages such as high-purity, homogeneity and precise composition relative to the conventional solid-state method which usually results in low surface area due to the high-temperature heat-treatment.

Doping with metal or nonmetal ion to $SrTiO_3$ material could extend its optical absorption edge towards the visible light range and generate the photo catalytic activity in visible light. The photo catalytic activity is not high application in visible light because of relatively large band gap energy of 3.2eV. Therefore, to extend the absorption range of strontium titanate towards the visible range is essential work to generate visible light responsive photo catalyst [13]. It is a great challenge to synthesize the catalyst which is active under visible light irradiation to use sun light. In commercial

multilayer ceramic capacitors (MLCs), perovskite structure titanates are frequently used as high permittivity dielectrics.

Owing to its high dielectric permittivity and its low microwave losses, it is the most attractive material for many high frequency and microwave applications. This material has been demonstrated to use as a high temperature oxygen sensor. $SrTiO_3$ is one of the promising photo catalyst material used in environmental applications [14].It was recently reported [15] that Ferro electricity can be induced, without an external electric field or pressure, in $SrTiO_3$ by the replacement of oxygen atoms. Also, it is considered to be applied as a promisingly tunable micro wave material due to its high performance under applied electric field. In general, the properties of perovskite-type materials depend mainly on the crystal size, defects, crystal surface and interface properties. For example, it has been found that the operation temperature of $SrTiO_3$ as an oxygen sensor can be lowered from 700°C to 40°C, when its grain size is reduced to the nanometer range, which lowers the required energy of the carriers to overcome the Schottky barriers. Generally, poly-dispersed and bulk $SrTiO_3$ have limited applications.

Strontium titanate-based ceramics have been widely used to produce some electronic components, such as grain boundary layer capacitors (GBLS), varistors, sensors, etc. $SrTiO_3$, cubic pervoskite-type crystal, has distinguished attention in its application in dielectric for dynamic random access memories (DRAM), because of high dielectric constant, lack of fatigue or aging problems in the working range, good thermal stability and high compatibility with device process. Strontium titanate is a promising compound, proving its usefulness in wide range of applications. It can be used as a grain boundary barrier layer capacitor, oxygen-gas sensor, substrate for the epitaxial growth of high temperature semiconductor thin film and as a catalyst. $SrTiO_3$, also has superconductivity when a small amount of electron carriers are added by oxygen vacancies [1].

1.2. Solid-State Reaction
A dry media reaction or solid-state reaction or solventless reaction is a chemical reaction system in the absence of a solvent. Reactions can take place between two solids. However, because of the relatively small diffusion rates in solids, the corresponding chemical reactions are very slow. They are accelerated by increasing the reaction temperature and finely dividing the reactant to increase the contacting surface area.

Solid State Reaction Route is the most widely used method for the preparation of polycrystallinesolids from a mixture of solid starting materials. Solids do not react together at room temperature over normal time scales and it is necessary to heat them to much higher temperatures, often to 1000°C to 1500°C in order for the reaction to occur at an appreciable rate. The factors on which the feasibility and rate of a solid state reaction include, reaction conditions, structural properties of the reactants, surface area of the solids, their reactivity and the thermodynamic free energy change associated with the reaction.

2. EXPERIMENTAL
Undoped and Nickel-doped (0.5% and 1% atom) Strontium titanates were prepared by solid-state reactions from strontium carbonate, titanium dioxide and nickel sulphate. All the powders had 99% purity. The powders were mixed in agate mortar using isopropyl alcohol up to dryness. Mixed powder was sintered at 1200°C for 1h and then milled again to destroy agglomerates. The sintered powder was characterized by XRD and showed a perovskite structure without evidence of additional phases.

3. RESULTS AND DISCUSSION
3.1. X-Ray Diffraction analysis
The X-ray diffraction spectra were recorded for undoped and Ni (0.5% and 1% atom) doped $SrTiO_3$ nanoparticles areshown in figure 1. All the diffraction peaks can be well indexed to the cubic pervoskite structure compared with undoped $SrTiO_3$, Ni doping on $SrTiO_3$ does not alter its pervoskite structure but there is a reduction observed at FWHM of the XRD patterns [2,5]. This reduction may be the result of the crystalline size-induced reduction or strain induced reduction since the positions of all distribution peaks almost unchanged as shown in figure 1, the strain induced reduction can be ignored therefore the reduction is purely due to the increased size of $SrTiO_3$ on Ni doping. The average grain size of undoped and Ni doped $SrTiO_3$ nano particles can be determine by Debye- Scherer formula,

$$D = \frac{K\lambda}{\beta Cos\theta} Å$$

The estimated average grain size of the particles is tabulated in table 3.1. The grain size obtained from Ni doped $SrTiO_3$ is bigger than the undoped $SrTiO_3$ crystals. Therefore Ni is an important dopant to improve the crystal growth. The lattice parameter (a) was calculated by selecting the (110) plane using the relation,

$$Sin^2\theta = \frac{\lambda^2}{4a^2}(h^2 + k^2 + l^2)$$

Table 1: Average grain sizes of the pure and Ni doped SrTiO$_3$ nanoparticles

Samples	2θ (deg)	FWHM (β)	Average GrainSize(nm)	Mean (nm)
Pure SrTiO$_3$	32.4089	0.1845	44.8	
	39.9568	0.1980	42.7	42.76
	46.4747	0.2122	40.8	
0.5% Ni-SrTiO$_3$	32.3758	0.1319	62.7	
	39.9338	0.1345	62.9	60.60
	46.4574	0.1539	56.2	
1% Ni- SrTiO$_3$	32.3879	0.1519	54.5	
	39.9377	0.1252	67.6	58.23
	46.4502	0.1644	52.6	

Table 2: The infrared absorption frequencies of pure and Ni doped SrTiO$_3$ nanoparticles

Frequencies (cm^{-1})			Tentative assignments
S$_1$ (PureSTO)	S$_2$ (0.5% Ni- STO)	S$_3$ (1% Ni - STO)	
-	-	3461	OH-stretching hydroxyl group
-	-	3434	OH-stretching
3293	-	-	OH- stretching
3271	-	-	OH- stretching
2917	2918	2915	C-H stretching methyl group
-	2850	-	Carbon-hydrogen stretching
-	1122	1123	Carbon-carbon stretching
-	-	1081	Carbon-carbon stretching
1019	1019	1019	C-O stretching
-	648	-	TiO$_6$ octahedron stretching vibration
-	582	589	Metal-oxygen bond
572	-	574	Metal-oxygen bond
-	-	564	Metal-oxygen bond
-	-	556	Titanium-oxide located
-	-	443	Ti-O bending normal vibration

From that the calculated value of a is 3.9038Å which is in good agreement with that of JCPDS – card no. 35–734.

3.2. Fourier Transform Infra-Red Spectroscopy

To examine the chemical bonding, FT-IR spectroscopy is a necessary tool to be used. The Figure 2 illustrates the FT-IR spectra of undoped and Ni doped (0.5% and 1% atom) SrTiO$_3$ samples. The structure of SrTiO$_3$ is further supported by the FT-IR spectra. The peaks around 3461 cm^{-1}–3271 cm^{-1} due to the absorption of O-H stretching indicating the presence of hydroxyl group. The weak absorption band at 2917 cm^{-1} and 2850 cm^{-1} represent the stretching modes of the methyl group and C-H of the aldehyde respectively. The C-C stretching modes of both acetaldehyde and crotonaldehyde occur in 1123 cm^{-1}–1081 cm^{-1} region. The absorption peak at ~ 443 cm^{-1} can be
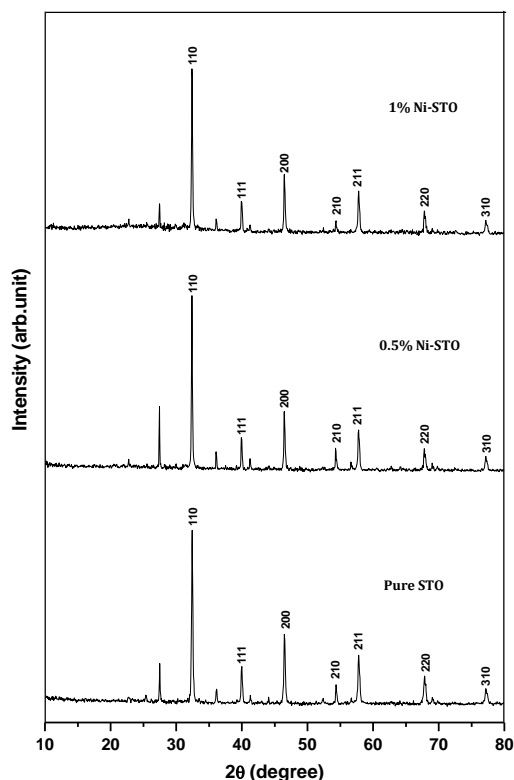
Figure 1: X-ray diffraction patterns of Pure and Nickel (0.5% and 1% atom) doped SrTiO$_3$ nanoparticles sintered at 1200 °C for 1h.

attributed to Ti-O bending vibrations. It may be noted that hear, the absorption peak corresponding to titanium oxide has been located at 556 cm^{-1}. On the contrary, the band representative to the metal oxygen bond is much more pronounced as it is indicated by the vibrations peaks from 589 cm^{-1}–564 cm^{-1}. The weak absorption at 648 cm-1 indicates the presence of TiO$_6$ octahedron stretching vibration. The absorption around 589 cm^{-1}–564 cm^{-1} is metal oxygen bond and the intensity of this peak could be seen to increase significantly with the increase in Ni ratio (0.5% & 1% atom). From the above results our investigations were well compared with earlier report that the weak bands observed around 589 cm^{-1}-564 cm^{-1} indicate the stretching modes of metallic oxygen bond [2,5,6,13-17]. The infrared absorption frequencies of pure and Ni doped SrTiO$_3$ nanoparticles are shown in table 2.

3.3. UV-Vis- DRS study

The UV-Vis diffuse reflectance spectra of Ni doped SrTiO$_3$ and undoped SrTiO$_3$ samples at room temperature are given in Figure 3. The absorption maximum decreases with the particle size [18]. As a comparison, the spectra of SrTiO$_3$, (0.5%) Ni-SrTiO$_3$ and (1%) Ni-SrTiO$_3$ were depicted in
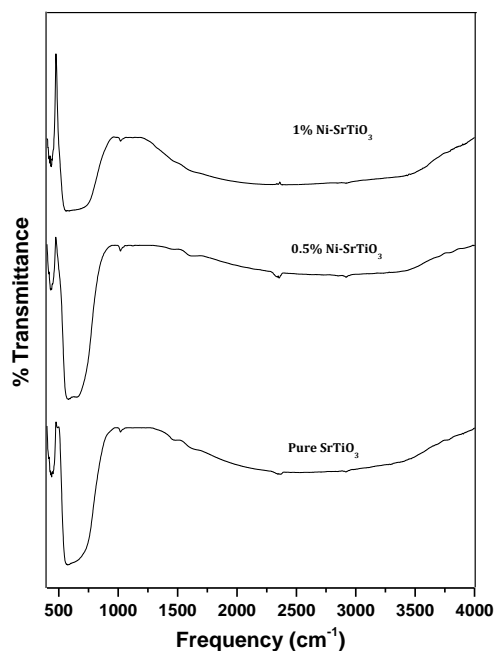

Figure 2: FTIR spectra of pure and Nickel (0.5% and 1% atom) doped SrTiO$_3$ nanoparticles.

Figure 3 from which it can be seen that the Ni doped SrTiO$_3$ as has almost identical absorption edge at ~ 300 nm to that of pure SrTiO$_3$. It has also been reported by [19]. However, a broad visible light absorption band, which indicates a high response to visible light, appears at around 520 nm in the UV-Vis spectra of Ni-SrTiO$_3$–1.0%, which is assigned to a transmission due to the level formed by Ni^{3+} ions [20]. The absorption intensity of (1%) Ni, SrTiO$_3$ was weaken than that of (0.5%) Ni–SrTiO$_3$ indicating that the formation of Ni^{3+} ions and was partly suppressed by dopant concentration as shown Figure 3.

The values of band gap energy for as synthesized samples increase with the (Ni) doping content increasing, revealing that the band gap energy was evidently increased by doping the material with Ni [5,16,17]. From the UV-Vis spectra the band gaps were calculated using the formula Eg = hC/ λ eV and are 3.67 eV, 4.13 eV and 4.46 eV respectively for undoped, 0.5% and 1% Ni doped SrTiO$_3$.

3.4. Scanning electron microscopy

Morphologies of as synthesized non-doped and Ni doped SrTio$_3$ (0.5% & 1%) were observed by SEM. As shown in Figure 4 to 3.6, the samples of SrTiO$_3$ and 0.5% Ni–SrTiO$_3$ and 1% Ni-SrTiO$_3$, prepared under the same condition but these possess an anomalous morphology. However the doped samples have given a more irregular structure and a greater particle size than that of
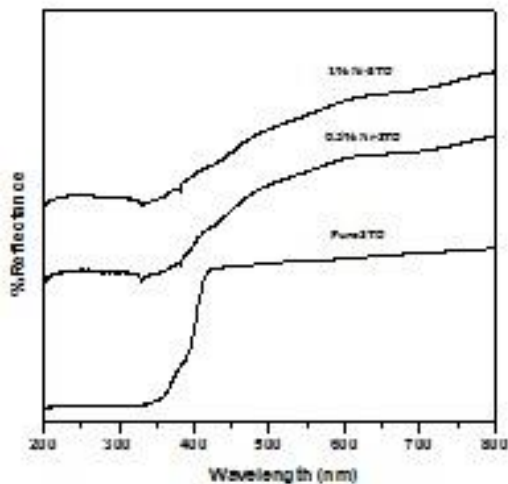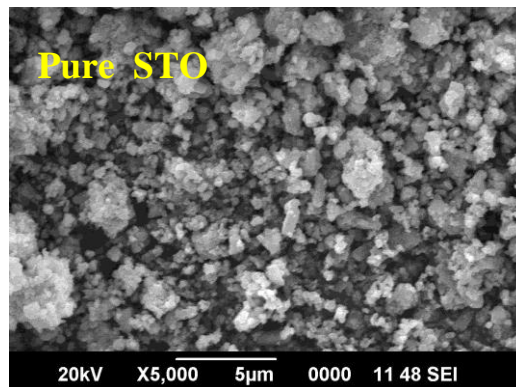
Figure 3: UV-Vis-Diffuse reflectance spectra of pureand Nickel doped SrTiO₃ nanoparticles.

Figure 4:SEM image of pure SrTiO₃ nanoparticles

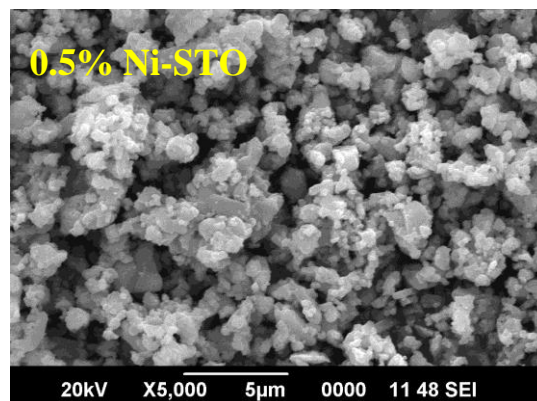**Figure 5:** SEM image of 0.5% Ni doped SrTiO₃nanoparticles

non-doped SrTiO₃. From Figures 4 to 6, it seems reasonable to believe that the decrease in particle size and rougher surface morphology are responsible for the increasing of surface area for doped samples; which was also reported in previous work on doping SrTiO₃ with often elements [3,21]. The smaller particle size of the doped ones can be explained by the fact that many crystal defects have been formed. When the dopant ions occupy regular lattice sites inside and for on the surface of SrTiO₃. As a result, the increase of surface defect inhibits the growth of the crystal, which has also been reported in previous work [22].

4. CONCLUSION

The Ni-doped SrTiO₃ pure and nanoparticleshad been successfully synthesized. Different experiments were performed to investigate the role of Nickel on the growth of SrTiO₃ nanomaterial. From X-ray diffraction peak position and relative strength, and the absorption performance on UV-Vis-DRS analysis revealed that the size of the SrTiO₃ was increased Ni doping has been increased to some extent than the undoped one particle size of Ni doped material is a slightly increased. From the morphology analysis, it is shown that the nano-sized particles in the precursor powder transform in to elongated plate-line (along a/b direction) grains, whereas no evident grain growth occurs along c direction. The combination of effective grain alignment and grain refinement opens up new possibilities for developing anisotropic ceramics with unique and improved performance. Ni doped sample have shown higher resistivity than undoped samples and that may be explained by the formation of thicker layer at the microstructure investigation, it is due to higher concentration of acceptor (Ni) doping.
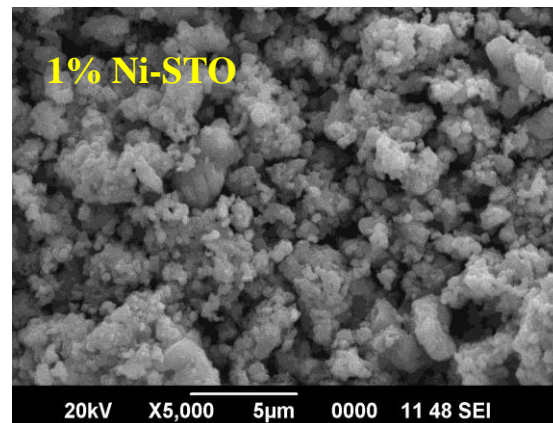
Figure 6:SEM image of 1%Ni doped SrTiO₃ nanoparticles

5. REFERENCES

[1]. G.Z.Cao., (2004) In: G.Z.Cao, Editor, Nanostructures and Nanomaterials: Synthesis, properties and Applications, *Imperial College Press,* London P, 331.

[2]. S.K.Rout, S. Panigrahi and J. Bera, (2005) Study on electrical properties of Ni-dopedSrTiO₃ ceramics using impedance

spectroscopy,***Bulletine of Material Science,*** **28**, 275–279.

[3]. Cristian-Daniel Savaniu, John T. S. Irvine, (2009) Reduction studies and evaluation of surface modified A-site deficient La-doped SrTiO$_3$ as anode material for IT-SOFCs. ***Journal of Materiel Chemistry,*** **19**, 8119-8128.

[4]. Denis J. Cumming, Vladislav V. Kharton, Aleksey A. Yaremchenko, Andrei V. Kovalevsky and John A. Kilner, (2011) Electrical Properties and Dimensional Stability of Ce-Doped SrTiO$_{3\_d}$ for Solid Oxide Fuel Cell Applications, ***Journal of American Ceramic Society,*** 1–8.

[5]. Nguyen Van Minh, Doan Thi Thuy Phuong, (2011) SrTiO$_{3x}$FeO$_3$ nanoparticle: a study of structural, optical, impedance and magnetic properties, ***Journal of Experimental Nanoscience,*** **6**, 3, 226-237.

[6]. Aizhong Jia, Zhiqian Su, Lan-Lan Lou and Shuangxi Lio, (2010) Synthesis and characterization of highly-active Nickel and Lanthanum Co doped SrTiO$_3$, ***Solid State Science,*** **12**, 1140-1145.

[7]. J. Gerblinger, H. Meixner,(1991) Fast Oxygen Sensors Based on Sputtered Strontium Titanate, ***Sensors and Actuators B,*** **4,** 99-102, 99.

[8]. Takuya Matsumoto, Tomoji Kawai, Katsuki Kitahama, Shichio Kawai, Ichiro Shigaki and Yoshio Kawate, (1991) Layer-by-layer epitaxial growth of a Bi$_2$Sr$_2$CuO$_6$ thin film on a Bi$_2$Sr$_2$CaCu$_2$O$_8$ single crystal, ***Applied Physics Letters,*** **58,** 2039.

[9]. E.A. Nenasheva, A.D. Kanareykin, N.F. Kartenko, A.I. Dedyk and S.F. Karmanenko, (2004) Ceramics Materials Based on (Ba,Sr)TiO$_3$ Solid Solutions for Tunable Microwave Devices, ***Journal of Electroceramics,*** **13,** 235–238.

[10]. Heyi Li, Leon Avery, Winfried Denk and George P. Hess, (1997) Identification of chemical synapses in the pharynx of Caenorhabditis elegans, ***Proc. Natl. Acad. Sci. USA,*** **94,** 5912–5916.

[11]. R.Hagenbeck, R.Waser, (1998) Influence of temperature and interface charge on the grain-boundary conductivity in acceptor-doped SrTiO$_3$ ceramics, ***Journal of Applied Physics,*** **83**, Issue:4, Pages: 2083-2092.

[12]. Jingchang Zhao, Xinghui Wu, Longtu Li, Xian Li, (2004) Preparation and electrical properties of SrTiO$_3$ ceramics doped with M$_2$O$_3$–PbO–CuO, ***Solid-State Electronics,*** **48**, 2287–2291.

[13]. M.A.F. De Souza, A. G, Souza, (2005) Synthesis and characterization of SrCo$_x$Ti$_{1-x}$O$_3$, ***Journal of Thermal Analysis and Calorimetry,*** **79**, 411-414.

[14]. Om Parkash, Devendra Kumar and C. Christopher, (2003) Preparation structure and dielectric behaviour of the system Sr$_{1-x}$La$_x$Ti$_{1-x}$Fe$_x$O$_3$ (x £ 0×50), ***Proceedings of Indian Academy of Sciences (Chem. Sci.),*** **115,** 649–661.

[15]. Y. S. Malghe., (2010) Nanosized SrTiO$_3$ powder from oxalate precursor microwave aided synthesis and thermal characterization, ***Journal of Thermo Analytical Calorimetry,*** **102,** 831–836.

[16]. Chia-Hao Chang, Yun-Hwei Shen, (2006) Synthesis and characterization of chromium doped SrTiO$_3$ photocatalyst, ***Materials Letters,*** **60**, 129-132.

[17]. Uyi Sulaeman, Shu Yin, Tsugio Sato, (2010)Microwave Assisted Solvothermal Synthesis and Visible Light Photocatalytic Properties of Nb and N Co-doped SrTiO3 Nanoparticles, ***Advances in Science and Technology***, **3**, 52-57

[18]. P.Calandra, M.Goffredi and V.T. Liveri, (1999) Study of the growth of ZnS nanoparticles in water/AOT/n-heptane microemulsions by UV-absorption spectroscopy, ***Colloid Surface. A,*** **160,** 9.

[19]. M. Miyauchi, M. Takashio, H. Tobimatsu, (2004) ***Langmuir*** **20**, 232,

[20]. R.Niishiro, H. Kato, A. Kudo, (2005) Nickel and Either Tantalum or Niobium-Codoped TiO2 and SrTiO3 PhotoCatalysts with Visible-Light Response for H2 or O2 Evolution from Aqueous Solutions***Physical Cheistry Chemical Physics,*** **7,** 2241-2245.

[21]. D.Wang, J. Ye, T. Kako, T. Kimura, (2005) ***Journal of Physical Chemistry. B,*** **110,** 15824.

[22]. Y.Qin, G. Wang, Y. Wang, (2007) ***Catalasis Communications,*** **8,** 926.